Title
De novo biosynthesis of terminal alkyne-labeled natural products

Journal
Nature Chemical Biology, 11(2)

ISSN
1552-4450

Authors
Zhu, Xuejun
Liu, Joyce
Zhang, Wenjun

Publication Date
2015-02-01

DOI
10.1038/nchembio.1718

Peer reviewed

De novo biosynthesis of terminal alkyne-labeled natural products

Xuejun Zhu[1,2], Joyce Liu[2,3], Wenjun Zhang[1,2,4*]

[1]Department of Chemical and Biomolecular Engineering, [2]Energy Biosciences Institute, [3]Department of Bioengineering, University of California, Berkeley, CA 94720, USA. [4]Physical Biosciences Division, Lawrence Berkeley National Laboratory, Berkeley, CA 94720, USA.

*e-mail:wjzhang@berkeley.edu

Abstract:

The terminal alkyne is a functionality widely used in organic synthesis, pharmaceutical science, material science, and bioorthogonal chemistry. This functionality is also found in acetylenic natural products, but the underlying biosynthetic pathways for its formation are not well understood. Here we report the characterization of the first carrier protein-dependent terminal alkyne biosynthetic machinery in microbes. We further demonstrate that this enzymatic machinery can be exploited for the *in situ* generation and incorporation of terminal alkynes into two natural product scaffolds in *E. coli*. These results highlight the prospect for tagging major classes of natural products, including polyketides and polyketide/non-ribosomal peptide hybrids, using biosynthetic pathway engineering.

Natural products are important small molecules widely used as drugs, pesticides, herbicides, and biological probes. Tagging natural products with a unique chemical handle enables the visualization, enrichment, quantification, and mode of action study of natural products through bioorthogonal chemistry[1-4]. One prevalent bioorthogonal reaction is the triazole-forming azide-alkyne [3+2] cycloaddition, often referred to as "click" chemistry[5]. This reaction has enabled selective imaging and study of azide- or alkyne-labeled glycans, proteins, nucleic acids and lipids. Despite the success with macromolecules, the labeling of natural products has not been adequately explored. It is often challenging to obtain tagged natural products through total synthesis because of their structural complexity, or through semi-synthesis because of their chemical lability and the limited supply of most natural products. Alternatively, precursor-directed biosynthesis (PDB) may be employed to produce azide- or alkyne-labeled natural products based on the promiscuity of biosynthetic machinery. Mainly used as a tool to introduce structural diversity, PDB has allowed us and other researchers to generate labeled natural products[3,6-8]. However, the coexistence of diffusible precursors and final products[9] with the same chemical handle introduces significant background in the PDB production system, making it incompatible with *in situ* bioorthogonal chemical transformations. We report here the *de novo* biosynthesis of alkyne-labeled natural products without the feeding of alkynoic precursors by characterizing and engineering the novel terminal alkyne synthetic machinery that living systems offer.

Many acetylenic natural products contain a terminal alkyne functionality, which seems to be crucial for their bioactivity (**Fig. 1**)[10,11]. Terminal alkynes can be formed by acetylenases, a special family of desaturases that catalyze O_2-dependent dehydrogenation of C-C bonds in a di-iron dependent mechanism[12]. Several membrane-bound acetylenases have recently been

identified from plants, insects, fungi, and bacteria[4,10,13-17], but all of these reports have been limited to bioinformatics or *in vivo* studies through mutagenesis or heterologous expression in yeasts and plants because it is notoriously difficult to work with the membrane-bound desaturases *in vitro*. As a result, no definitive information on the reactions catalyzed by these enzymes is available to date. Regardless of these challenges, a thorough characterization of terminal alkyne biosynthetic machinery, particularly the substrate specificity, is the indispensable first step for utilization of these enzymes in the biosynthesis of alkyne-labeled natural products.

While the genetic basis for the synthesis of most acetylenic natural products is yet to be determined, two gene clusters have been identified to be responsible for the synthesis of jamaicamides and carmabins (**Fig. 1**), which are terminal alkyne-bearing polyketide/non-ribosomal peptide (PK/NRP) hybrids from the marine cyanobacteria *Moorea producens* (formerly classified as *Lyngbya majuscula*)[18,19]. These findings serve as a starting point for studying the enzymatic machinery involved in the biosynthesis of terminal alkynes residing in PK/NRP molecular scaffolds. It is proposed that the alkyne functionality of jamaicamide is introduced as a short-chain alkynoic starter unit by a three-gene operon: *jamABC* encoding a homolog of a fatty acyl-CoA ligase, a membrane-bound fatty acid desaturase, and an acyl carrier protein (ACP), respectively. A tri-gene cassette *camABC* highly homologous to *jamABC* has also been identified in the biosynthetic gene cluster of carmabins, suggesting a conserved biosynthetic logic in generating the terminal alkyne functionality in both families of compounds. JamA particularly prefers 5-hexynoic and 5-hexenoic acid vs. other saturated fatty acids in the ATP-PP_i exchange assay[18], indicating that the JamB-mediated desaturation may occur prior to activation by JamA, on the free hexanoic acid. However, fatty acids with varying saturation levels (hexanoic, 5-hexenoic, and 5-hexynoic acid) can be loaded onto JamC upon activation by

JamA[20], raising questions about the native substrate and reaction timing of JamA and JamB. The use of a free fatty acid or ligation of a C_6 starter to the ACP prior to dehydrogenation would be unexpected as membrane desaturases typically accept CoA or glycerolipid substrates[12,21].

Here we elucidated the functions of JamA, B, and C in the biosynthesis of terminal alkyne functionality of jamaicamide by both *in vitro* and *in vivo* analyses. JamB was demonstrated to be a carrier protein-dependent membrane-bound acetylenase/desaturase with stringent substrate specificity towards both the acyl group and the acyl carrier. The terminal alkyne biosynthetic gene cassette was further co-expressed with biosynthetic genes of two different natural products in *E. coli* for generating terminal alkyne-labeled PK and PK/NRP hybrid without the feeding of alkynoic precursors.

RESULTS

Reconstitution of JamABC activities *in vitro*

To probe the activity of JamABC in terminal alkyne formation, we overexpressed each gene in *E. coli* and purified JamA, JamC, and the JamB-containing membrane fraction for use in biochemical assays (**Supplementary Results, Supplementary Fig. 1)**. The membrane fraction purified from the *E. coli* strain transformed with an empty vector was prepared in parallel and used as a negative control in JamB assays. We first tested the requirement of a thio-carrier for JamB using substrates that included 5-hexenoic acid, 5-hexenoyl-CoA, and 5-hexenoyl-JamC. We synthesized 5-hexenoyl-CoA enzymatically using ORF35, a promiscuous acyl-CoA ligase that we recently identified[22]. 5-Hexenoyl-JamC (**1**) was prepared *in situ* using an enzymatic reaction containing JamA, JamC, and 5-hexenoic acid[20]. While JamB failed to act on 5-hexenoic acid or 5-hexenoyl-CoA (**Supplementary Fig. 2 and 3**), 5-hexenoyl-JamC was converted by

JamB to 5-hexynoyl-JamC (**2**) as detected by liquid chromatography-high-resolution mass spectrometry (LC-HRMS) analysis (**Fig. 2, a, b and c**). Product identity was further confirmed by comparison to authentic **2** synthesized using the enzymatic reaction containing JamA, JamC, and 5-hexynoic acid[20]. Control experiments demonstrated that the formation of **2** relied on the presence of both JamB and **1**. We were able to observe the activity of JamB without the addition of an electron transport system and reducing equivalents, indicating that these presumably essential components were provided at least to some extent by the partially purified JamB-containing membrane fraction from *E. coli*[23]. Indeed the introduction of ferredoxin, ferredoxin reductase, and NADPH slightly increased the activity of JamB (by ~35%), suggesting that the reduced ferredoxin is a likely electron donor for the JamB-catalyzed desaturation reaction. This result is consistent with observations that in cyanobacteria, membrane-bound desaturases typically use ferredoxin instead of cytochrome b_5 as an electron transport partner[23-25], and ferredoxin is often a required cofactor for soluble acyl-ACP desaturases[26]. We thus confirmed JamB to be the first terminal acetylenase/desaturase that functions in a microbial polyketide synthase (PKS)/non-ribosomal peptide synthetase (NRPS) pathway to install a terminal alkyne functionality. It is notable that JamB is also the first exception to the conventional view that only soluble desaturases work on acyl-ACPs while membrane desaturases utilize acyl-CoAs or lipids as substrates[12,21,27].

Substrate specificity of JamB

Since bifunctional desaturases have been observed to catalyze alkyne formation from a saturated fatty acyl chain through a four-electron oxidation[12], we first examined the activity of JamB on hexanoyl-JamC. The conversion from hexanoyl-JamC to 5-hexynoyl-JamC was undetectable; instead we observed the formation of 5-hexenoyl-JamC in a trace amount catalyzed by JamB

(**Supplementary Fig. 4**). We next probed the acyl chain length specificity of JamB. Alkenoyl moieties ranging in the chain length from five to eight carbons were enzymatically linked to JamC using the promiscuous JamA[18] (4-pentenoyl-JamC and 6-heptenoyl-JamC) (**Supplementary Fig. 5** and **6**) or a phosphopantetheinyl transferase Sfp[28] (7-octenoyl-JamC) (**Supplementary Fig. 7**). JamB failed to convert these alkenoyl-JamCs to their corresponding alkynoyl-JamCs (**Fig. 3** and **Supplementary Fig. 5-7**), demonstrating the stringent chain length specificity of JamB. In addition, although JamA did not discriminate among fatty acid substrates with different unsaturation patterns such as 2-hexenoic, 3-hexenoic, and 4-hexenoic acid, LC-HRMS analyses of the enzymatic reaction mixtures of these hexenoyl-JamCs and JamB revealed no detectable formation of their corresponding hexynoyl-JamCs, suggesting that a terminal alkene functionality is required for JamB activity (**Fig. 3** and **Supplementary Fig. 8-10**).

In addition to the acyl moiety, we further scrutinized the ACP specificity of JamB. We purified three heterologous ACPs, including CamC (identity/similarity: 95/98%), scACP (identity/similarity: 8/15%) from *Streptomyces coeruleorubidus* NRRL 18370, and fsACP (identity/similarity: 10/19%) from *E. coli* BL21 (DE3). As JamA efficiently recognized CamC but not the other ACPs (**data not shown**), we synthesized the three corresponding 5-hexenoyl-ACPs using JamA, scFadD (a medium-chain fatty acyl-ACP synthetase homolog encoded in the same operon as scACP), and Sfp, respectively. The activity of JamB was observed towards 5-hexenoyl-CamC but not the other 5-hexenoyl-ACPs (**Fig. 3** and **Supplementary Fig. 11-13**), implying strong protein-protein interactions between the acetylenase/desaturase and the dedicated ACP for terminal alkyne synthesis. Genome-mining analysis identified more than 80 gene clusters encoding homologs of *jamABC* across diverse bacterial genera (**Supplementary Fig. 14**), suggesting that the carrier protein-dependent alkyne biosynthetic pathway is

widespread in bacteria. The functions and substrate specificities of these homologs are yet to be determined.

Engineered biosynthesis of alkyne-tagged natural products

Elucidation of the functions of JamABC in generating a thio-activated, short-chain alkynoic moiety defines a portable tri-gene cassette that can be utilized for *in situ* generation and incorporation of terminal alkynes into various molecular scaffolds through biosynthetic pathway engineering. To apply this newly characterized enzymatic machinery in *E. coli*, we first targeted the biosynthesis of terminal alkyne-bearing polyketides through starter unit engineering. We selected a type III polyketide synthase HsPKS1 from the plant *Huperzia serrata* to assemble polyketide backbones using malonyl-CoA extender units. HsPKS1 is able to accept a variety of starter units including aromatic and aliphatic (C_6-C_{10}) CoA thioesters[29], suggesting that the recognition of the 5-hexynoyl starter unit would be likely. Two plasmids encoding *jamABC* and *hspks1*, with each gene regulated by a T7 promoter, were transformed into the *E. coli* BAP1 strain[30] yielding the strain XZ1 (**Supplementary Fig. 15**). We omitted either *jamA, B, C,* or *hspks1* individually to yield four control strains. The resulting strains were grown in shake flask cultures, and after induction with IPTG, the strains continued to grow in F1 minimal medium supplemented with 5-hexenoic acid at 20 °C for two days. Analyses of these culture extracts by HPLC and LC-HRMS revealed the production of a putative alkyne-labeled polyketide **3** by XZ1 at ~0.3 mg/L (**Fig. 4**) which is comparable to the typical polyketide titer in *E. coli* using similar culture conditions[31]. The product **3** was later revealed to be a novel pyrone with the retention time, UV spectrum, and mass patterns precisely matching those of the standard synthesized by a scaled-up enzymatic reaction of HsPKS1 using the 5-hexynoyl starter unit (**Supplementary Table 3 and Supplementary Fig. 16** and **17**). **3** was presumably formed by condensing the 5-

hexynoyl moiety with two malonyl-CoAs followed by a spontaneous intramolecular cyclization. It is notable that in addition to **3**, a major byproduct **4** bearing a terminal alkene functionality retained from the fed alkene precursors was also produced (**Fig. 4** and **Supplementary Fig. 18**)[32]. **3** and **4** were made in a ~1:4 ratio; this efficiency was mostly likely dictated by the non-optimized activity of the membrane-bound acetylenase/desaturase JamB in this heterologous host as HsPKS1 showed no preference towards 5-hexenoyl and 5-hexynoyl starter units.

The production of **3** by XZ1 co-expressing *jamABC* and *hspks1* confirmed the function of this tri-gene cassette (*jamABC*) in the model organism *E. coli*, and demonstrated the feasibility of *de novo* synthesizing terminal alkyne-labeled natural products by starter unit engineering. Omitting JamC completely abolished the production of **3** as determined by HPLC and the much more sensitive LC-HRMS analyses (**Fig. 4** and **Supplementary Fig. 16**), which further confirmed the necessity of this carrier protein for the desaturation activity of JamB. Deletion of JamA decreased the titer of **3** by ~30-fold as shown by selected MS ion monitoring (**Supplementary Fig. 16**), indicating endogenous acyl-ACP synthetases of *E. coli* could complement the activity of JamA, albeit with a much lower efficiency. In addition, the reported broad substrate specificity of HsPKS1 rendered the engineered *E. coli* strain XZ1 an excellent reporting system for further probing the fatty acyl substrate specificity of JamB. We fed selected fatty acids, such as 4-pentenoic, 6-heptenoic, and 7-octenoic acids, to the *E. coli* cultures, and analyzed culture extracts by both selected MS ion monitoring and MS-based comparative metabolomics between XZ1 and negative control strains without *jamB*. This extensive analysis revealed that XZ1 failed to produce alkyne-tagged products using these precursors (**Supplementary Fig. 19-21**), consistent with the *in vitro* biochemical results showing the strict substrate specificity of JamB.

We next explored extender unit engineering, an alternative strategy for incorporating an alkynoic extender unit into the molecular scaffolds of PKs. Although the majority of PKs utilize malonyl-CoA or methylmalonyl-CoA as extender units, longer-chain fatty acyl extender units have been identified in a few modular assembly lines[33]. We recently scrutinized the biosynthetic machinery for antimycin-type depsipeptides and identified a minimum set of enzymes (AntCDEFGM) required for generation of the antimycin dilactone scaffold[34]. The hybrid NRPS/PKS assembly line features the formation and incorporation of atypical PKS extender units by the actions of a reductase/carboxylase homolog AntE and an acyltransferase (AT) domain embedded in AntD. It has been shown that an alkynoic extender unit can be recognized by the promiscuous AntE and AntD-AT to synthesize an alkyne-labeled antimycin by PDB in *Streptomyces*[8]. In order to eliminate the requirement of alkynoic precursors and *de novo* biosynthesize alkyne-tagged antimycin analogues, we co-expressed *antCDEFGM* and *jamABC* in the *E. coli* BAP1 strain (**Supplementary Fig. 22**), which led to the production of antimycin-type depsipeptides at ~0.2 mg/L. A major alkyne-bearing antimycin analogue **5** was produced with a retention time and mass fragmentation patterns matching those of the standard synthesized through PDB (**Fig. 5**, **Supplementary Table 4 and Supplementary Fig. 23**). As expected, the deletion of *jamB* or *antC* completely abolished the production of **5** (**Fig. 5b**). The biosynthesis of **5** suggested that 5-hexynoyl-JamC could enter *E. coli* fatty acid metabolic pathways for additional processing.

DISCUSSION

Despite the importance of terminal alkyne and its prevalence in synthetic compounds, the biological routes to this functionality are not well understood until now. In this study, the biochemical characterization of JamA, B, and C resulted in a sequence of chemical steps in

generating the hexynoic starter unit for jamaicamides: 5-hexenoic acid is activated with ATP and loaded onto JamC by JamA, and then modified by JamB to form a terminal alkyne moiety before the priming of the PKS (**Fig. 2a**). This carrier protein-dependent terminal alkyne biosynthetic mechanism is likely adopted in generating a variety of acetylenic natural products, such as polyynes, since the most recently identified polyyne biosynthetic gene clusters contain genes encoding a fatty acyl-AMP ligase and an ACP in proximity with those encoding desaturases[4,16]. In addition, although a terminal alkene was shown to be essential for JamB-catalyzed alkyne synthesis in the biochemical analysis and *E. coli* feeding studies, we could not rule out the possibility of hexanoic acid as the starting substrate for the system of JamABC in *Moorea producens* based on the substrate promiscuity of JamA and JamB towards the saturated acyl chain.

Desaturase enzymes have evolved independently twice: the widespread integral membrane desaturases are found in endomembrane systems in both prokaryotes and eukaryotes, whereas the soluble acyl-ACP desaturases are found in plastids of higher plants[12]. The conjugation of the substrate to an ACP prior to desaturation is unusual for a membrane-bound desaturase, and JamB has a sequence surprisingly reminiscent of a microsomal eukaryotic desaturase with 48% amino acid similarity to the *Saccharomyces cerevisiae* Ole1p Δ^9-desaturase despite its prokaryote origin. Since plastids are hypothesized to be a result of an endosymbiotic event where early photosynthetic prokaryote invaded a primitive eukaryotic host[35], the use of ACP in a prokaryotic context, although with few examples, can be explained from an evolutionary view. By analogy to soluble acyl-ACP desaturases, three conserved His boxes (HX_4H, HX_2HH, and QX_2HH) are found in JamB and probably include the ligands for a diiron cluster at the catalytic site of the enzyme (**Supplementary Fig. 1**)[21,36]. It is interesting that

although the sequence of JamB is distinct from the known Δ^5-desaturases from plants, fungi, and humans, the third His box domain in JamB aligns with the consensus sequence of Δ^5-/Δ^6-desaturases (QX_2HH), consistent with the regiospecificity of JamB. Unlike the soluble desaturase that has a deep binding cavity into which substrates enter in an extended conformation, the membrane-bound desaturase has been suggested to have active site architecture with a cleft into which substrates enter laterally. However, the lack of a membrane desaturase crystal structure limits the mechanistic understanding of this family of enzymes[12]. Furthermore, in comparison with a typical desaturase involved in double bond formation, how an acetylenase abstracts two hydrogens from adjacent carbon atoms linked by a double bond without forming an epoxide remains an intriguing mechanistic question.

The characterization of JamA, B, and C enabled the *de novo* biosynthesis of terminal alkyne-labeled natural products through pathway engineering in absence of an alkynoic precursor. Two different strategies, starter and extender unit engineering, have been shown to be successful in labeling natural products based on the promiscuity of PKS/NRPS enzymatic machinery. Starter unit engineering could be generalized to tag polyketides and lipopeptides that naturally contain fatty acyl starter units, and extender unit engineering using *jamABC*, *antE*, and *antD-AT* in other modular assembly lines could lead to the site-selective introduction of a terminal alkyne into additional PKs or PK/NRP hybrids inside living cells. We have thus built a molecular toolbox that can be adapted to install a terminal alkyne functionality in a range of natural products. Although JamB appeared to have stringent substrate specificity and limited efficiency in *E. coli*, screening additional homologous gene cassettes from a large collection identified through genome-mining may yield new enzyme candidates with altered substrate specificities and improved efficiency in a targeted production organism (**Supplementary Fig.**

14).

In summary, we have provided direct evidence for the first ACP-dependent terminal acetylenase/desaturase responsible for terminal alkyne synthesis by both *in vitro* and *in vivo* analyses. We have further demonstrated that this biosynthetic pathway can be exploited for the *in situ* generation and incorporation of terminal alkynes into different natural products in *E. coli*. In addition to directly producing orthogonally functionalized natural product analogues that can be subjected to facile chemical modification for drug screening, our work may significantly advance the field of natural product research through coupling with diverse azido analytical handles. For example, using a fluorogenic probe[37,38], *in situ* detection and quantification of natural products in producing cell cultures can be accomplished for the first time. Furthermore, since azide-alkyne click chemistry continues to serve as a powerful tool in drug discovery and chemical biology[5,39,40], our findings open the door to numerous biological applications in which *in situ* enzymatic generation of a terminal alkyne is required or preferred.

Acknowledgement

This research was financially supported by the Pew Scholars Program and University of California Cancer Research Coordinating Committee funds. We thank I. Abe (the University of Tokyo) for providing *hspks1*, S. Bauer (UC Berkeley) for assisting with LC-HRMS analysis, J. Pelton (UC Berkeley) for helping with NMR spectroscopic analysis, J. Chung (UC Berkeley) for helping with compound purification, and L. Zhang (UC Berkeley) for providing scACP.

Author Contributions

X. Z. designed the experiments, performed all experiments, analyzed the data and wrote the manuscript.

J. L. constructed plasmids for antimycin production in *E. coli*.

W. Z. designed the experiments, analyzed the data and wrote the manuscript.

Competing financial interests

The authors declare no competing financial interests.

Additional information

Supplementary information and chemical compound information are available in the online version of the paper. Reprints and permissions information is available online at http://www.nature.com/reprints/index.html. Correspondence and requests for materials should be addressed to W. Z. (wjzhang@berkeley.edu).

Figure legends

Figure 1. Examples of acetylenic natural products with a terminal alkyne functionality.

Figure 2. Biochemical characterization of JamA, B, and C. (a) The biosynthetic pathway for the C_6 alkynoic starter unit generation and incorporation into jamaicamide B. (b) LC-HRMS chromatograms showing that 5-hexenoyl-JamC (**1**) was converted by JamB to 5-hexynoyl-JamC (**2**) (trace ii) with a retention time and mass matching those of the **2** standard (trace i). **2** was undetectable in controls without JamB (trace iii) or **1** (trace iv). (c) Deconvoluted masses of **1** and **2** in HRMS analysis. At least three independent replicates were performed for each assay, and representative results are shown.

Figure 3. Substrate specificity of JamB. At least three independent replicates were performed for each assay.

Figure 4. Biosynthesis of **3** through starter unit engineering. (a) Schematic of **3** formation in *E. coli*. (b) HPLC analysis (285 nm) showing the production of **3** upon co-expression of *jamABC* and *hspks1* (trace i). **4** was the major byproduct upon the feeding of 5-hexenoic acid. The standards of **3** and **4** were synthesized *in vitro* by large-scale enzymatic reactions (trace vi and vii). The absence of *jamA* (trace ii), *jamB* (trace iii), *jamC* (trace iv), or *hspks1* (trace v) significantly decreased or abolished the production of **3**. At least three independent replicates were performed, and representative results are shown; $P<0.01$.

Figure 5. Biosynthesis of **5** through extender unit engineering. (a) Schematic of **5** formation in *E. coli*. C, condensation; A, adenylation; T, thiolation; KR, ketoreduction; KS, ketosynthase; AT, acyltransferase; ACP, acyl carrier protein; TE, thioesterase. (b) Extracted ion chromatograms showing the production of **5** upon co-expression of *jamABC* and *antCDEFGM* (trace i). The

standard of **5** was synthesized by feeding 7-octynoic acid (trace ii). Deletion of *jamB* (trace iii) or *antC* (trace iv) completely abolished the production of **5**. The calculated mass (m/z =417.2020 $[M+H]^+$) with a 10 ppm mass error tolerance was used. At least three independent replicates were performed, and representative results are shown.

Online methods

Materials. Phusion High-Fidelity PCR Master Mix (NEB) was used for PCR reactions. Restriction enzymes were purchased from Thermo Scientific. 2-Hexenoic (purity 96%), 3-hexenoic (purity 97%), 4-hexenoic (purity 98%), 5-hexenoic (purity 99%), 5-hexynoic (purity 97%), 6-heptenoic (purity 98%) acids were purchased from Alfa Aesar. Hexanoic (purity >99.5%), 4-pentenoic (purity 97%), 4-pentynoic (purity 95%), 6-heptynoic (purity 90%), 7-octenoic (purity 97%) acids were purchased from Sigma Aldrich. 7-Octynoic acid (purity 95%) was obtained from AfferChem, Inc, NJ, USA. ^{13}C-1,3-labeled malonic acid, *d6*-DMSO, and *d4*-methanol were purchased from Cambridge Isotope Laboratories, Inc. LB medium was purchased from EMD Chemicals. Other chemicals were obtained from Alfa Aesar or Sigma Aldrich.

Bacterial strains, plasmids and DNA manipulations. *JamA, B,* and *C* were synthesized individually without codon optimization from gBlocks (IDT), *camC* was synthesized from GenScript with codon optimization for expression in *E. coli*. *Hspks1* was provided by I. Abe (the University of Tokyo). *AntD, GF,* and *M* were PCR amplified from genomic DNA extracted from *Streptomyces albus*. *AntE* was PCR amplified from genomic DNA extracted from *Streptomyces ambofaciens*. *AntC* was digested from the pET30-antC plasmid using NdeI and XhoI. *ScFadD* and *scACP* (Accession number: KJ950369) were PCR amplified from genomic DNA extracted from *Streptomyces coeruleorubidus* NRRL 18370. *FsACP* (Accession number: CAQ31615) was PCR amplified from *E. coli* BL21 (DE3). *JamA* and *jamC* were assembled together as *jamAC* by overlapping extension PCR with primers pXZ48_F_NcoI, pXZ48_R, pXZ48_F, and pXZ43_R_BamHI. *JamAC* was then ligated into pETDuet-1. Plasmid constructions were performed using standard protocols. Plasmids were purified from *E. coli* XL1-Blue with a QIAprep Spin Miniprep Kit and confirmed by DNA sequencing.

Protein expression and purification. All soluble proteins purified in this work contained *C*- or *N*- terminus hexahistidine tags. The expression plasmids were transformed into *E. coli* BL21 (DE3) or BAP1 for protein expression. The cells were grown at 37 °C in 750 mL of LB medium with appropriate concentrations of antibiotics to an OD_{600} of 0.4-0.6. The cells were induced with 0.1 mM isopropyl-β-D-thiogalactopyranoside (IPTG) for 16 h at 16 °C. The cells were harvested by centrifugation (4424 × g, 15 min, 4 °C), resuspended in 30 mL of lysis buffer (50 mM HEPES, pH=8.0, 300 mM NaCl, 10 mM imidazole) and lysed by homogenization on ice. Cell debris was removed by centrifugation (15,000 × g, 1 h, 4 °C). Ni-NTA agarose resin was added to the supernatant (1.5 mL/L of culture) and the solution was nutated at 4 °C for 1 h. The protein-resin mixture was loaded onto a gravity flow column, and proteins were eluted with increasing concentrations of imidazole in buffer A (50 mM HEPES, pH=8.0, 300 mM NaCl). Purified proteins were concentrated and buffer exchanged into HEPES buffer (50 mM HEPES, pH=8.0, 100 mM NaCl) with Amicon Ultra filters. The final proteins were flash-frozen in liquid nitrogen and stored at -80 °C. Protein concentrations were determined by NanoDrop. The approximate protein yields were 2.3 mg/L JamA (67 kDa), 4.0 mg/L JamC (12 kDa), 4.3 mg/L CamC (13 kDa), 26.9 mg/L scFadD (56 kDa), 4.5 mg/L scACP (11 kDa), 10 mg/L fsACP (10 kDa).

For JamB expression and purification, plasmid pXZ34 (*jamB* in pETDuet-1) or the empty pETDuet-1 vector was transformed into *E. coli* BL21 (DE3) cells. The cells were grown at 37 °C in 750 mL of LB medium with 100 μg/mL carbenicillin to an OD_{600} of 0.4. The cells were then induced with 0.1 mM IPTG for 16 h at 16 °C. The cells were harvested by centrifugation (4424 × g, 15 min, 4 °C), resuspended in 30 mL of HEPES buffer (50 mM HEPES, pH=8.0, 100 mM NaCl) and lysed by homogenization on ice. Cell debris was removed by centrifugation

(10,000 × g, 10 min, 4 □C). The supernatant was further ultracentrifugated (100,000 × g, 1 h, 4 □C) to collect the cell membrane. The membrane fraction was used in the *in vitro* assays immediately or stored at -80 □C.

Enzymatic synthesis and purification of 5-hexenoyl-CoA and 7-octenoyl-CoA. For the generation of acyl-CoAs, a typical reaction mixture contained 50 mM HEPES (pH 8.0), 2 mM $MgCl_2$, 2 mM ATP, 5 mM fatty acids, 2 mM CoA. The reactions were initiated by the addition of 10 μM Orf35. The reaction was quenched with the addition of trichloroacetic acid (TCA) to a final concentration of 5% (v/v). Precipitated proteins were removed by centrifugation. 5-Hexenoyl-CoA was purified from the supernatant by reverse-phase HPLC through an Intertsil ODS-4 column (4.6 mm i.d., 250 mm L, GL Sciences Inc.) with a linear gradient of 2-95% CH_3CN (v/v) over 20 min followed by 5 min in 95% CH_3CN with 0.1% (v/v) trifluoroacetic acid (TFA) at a flow rate of 1 mL/min. Fractions containing the alkenoyl-CoAs were collected manually, concentrated under vacuum, and dried to white solid using a lyophilizer.

JamB activity assay on acyl-ACPs. For the generation of acyl-JamCs, CamC, and scACP, a typical 100 μL of reaction mixture contained 50 mM HEPES (pH 8.0), 1 mM $MgCl_2$, 1 mM TCEP, 2 mM ATP, 1 mM fatty acids, and 100 μM holo-JamC, holo-CamC, or holo-scACP. The reactions were initiated by the addition of 5 μM JamA or scFadD. For the generation of 5-hexenoyl-fsACP and 7-octenoyl-JamC, a typical 100 μL of reaction mixture contained 50 mM HEPES (pH 8.0), 1 mM $MgCl_2$, 1 mM TCEP, 2 mM ATP, 1 mM 5-hexenoyl-CoA or 7-octenoyl-CoA, and 100 μM apo-fsACP or apo-JamC. The reactions were initiated by the addition of 5 μM Sfp. All of the reactions were incubated at room temperature for 2 h, and then further processed in the JamB activity assay. Particularly, 0.1 mM $Fe(NH_4)_2(SO_4)_2$, 500 u of catalase, and 100 μg of the JamB-containing membrane fraction or the membrane fraction purified from the *E. coli* strain

transformed with an empty vector were added to the reaction mixtures. For the assay with ferredoxin system, 10 μg of ferredoxin and 0.5 u/mL ferredoxin reductase and 0.4 mM NADPH (or 100 μM sodium dithionite was used to replace ferredoxin reductase and NADPH) were also added into the reaction mixture. The membrane fraction was removed by centrifugation (21,000 × g, 4 □C) after 20 min of incubation. The supernatant was then diluted to a final concentration of 1 μM of ACP, which was processed by nanocapillary LC-HRMS analysis using a chip column (Agilent Zorbax 300SB-C18 5 μm; separation, 43 mm × 75 μm; enrichment, 4 mm 40 nL) in-line with a QTOF (Agilent 6510 Q-TOF LC/MS). A linear gradient of 3–70% CH_3CN over 60 min in H_2O with 0.1% formic acid at a flow rate of 0.6 μL/min was used for analysis. MassHunter Qualitative Analysis software was used to analyze data, and the intact protein masses were obtained using a maximum entropy deconvolution algorithm (mass range: 10,000-17,000 daltons, minimum consecutive charge states: 5, minimum protein fit score: 8). At least three independent replicates were performed for each assay, and representative results are shown.

JamB activity assay on 5-hexenoyl-CoA. 100 μg of the JamB-containing membrane fraction or the membrane fraction purified from the *E. coli* strain transformed with an empty vector was incubated with 50 mM HEPES (pH 8.0), 1 mM $MgCl_2$, 1 mM TCEP, 2 mM ATP, 5 mM 5-hexenoyl-CoA, 0.1 mM $Fe(NH_4)_2(SO_4)_2$, and 500 u of catalase for 20 min. The reaction was quenched by the addition of TCA to a final concentration of 5% (v/v). Precipitated proteins were removed by centrifugation. LC-HRMS analysis was performed on an Agilent Technologies 6520 Accurate Mass QTOF LC-MS with an Agilent Eclipse Plus C18 column (4.6 × 100 mm) using a linear gradient of 2-98% CH_3CN (v/v) over 20 min followed by 10 min in 98% CH_3CN supplemented with 0.1% (v/v) formic acid at a flow rate of 0.5 mL/min. At least three independent replicates were performed for each assay, and representative results are shown.

JamB activity assay on 5-hexenoic acid. A typical reaction contained 50 mM HEPES (pH 8.0), 5 mM 5-hexenoic acid, 1 mM $MgCl_2$, 2 mM ATP, 1 mM TCEP, 0.1 mM $Fe(NH_4)_2(SO_4)_2$, 500 u of catalase, and 100 μg of the JamB-containing membrane fraction or the membrane fraction purified from the *E. coli* strain transformed with an empty vector. The 50 μL reaction was quenched by the addition of 6.5 μL 10% (w/v) NaCl and 6.5 μL glacial acetic acid. Fatty acids were extracted by the addition of 50 μL ethyl acetate. Methyl esters were generated using a standard protocol[41]. 25 μL of the supernatant was mixed with 225 μL of 30:1 (v/v) methanol and 37% HCl, and incubated at 45 °C for 1 h. After cooling to room temperature, 125 μL dH_2O and 125 μL hexanes were added. The mixture was vortexed and 50 μL supernatant was used for GC-MS analysis. Typical GC-MS analysis was conducted on a Varian CP-3800 instrument equipped with a Varian 320-MS using a Varian factorFOUR capillary column (30 m, 0.25 mm, DF = 0.25) and helium as the carrier gas (1 mL/min). The method ramped from 50 °C to 130 °C at 10 °C/min, and was further ramped to 300 °C at 40 °C/min. The mass patterns were compared to standards in the NIST library. At least three independent replicates were performed for each assay, and representative results are shown.

Genome mining analyses of *jamABC*. Genome mining analyses were performed using Integrated Microbial Genomes database (http://img.jgi.doe.gov/) with default parameters.

Biosynthesis of polyketides in *E. coli*. BAP1/pXZ30+pXZ43, BAP1/pXZ24+pXZ43, BAP1/pXZ27+pXZ34, BAP1/pXZ27+pXZ43, BAP1/pXZ27+pXZ44 cells were grown in 250 mL of LB medium with 100 μg/mL carbenicillin and 100 μg/mL spectinomycin at 37 °C to an OD_{600} of 0.4-0.6. Subsequently, the cells were harvested and concentrated 5-fold into 50 mL fresh F1 medium (1 L contains 3 g KH_2PO_4, 6.62 g K_2HPO_4, 4 g $(NH_4)_2SO_4$, 150.5 mg $MgSO_4$, 5 g glucose, 1.25 mL trace metal solution, 100 μM $Fe(NH_4)_2(SO_4)_2$, and 10 mL 100 × vitamin

solution) supplemented with 100 μg/mL carbenicillin, 100 μg/mL spectinomycin, 0.5 mM IPTG, and 1 mM alkenoic acid. After 48 h of growth at 20 °C, the culture broth and the cell pellets were separated by centrifugation. Polyketides were extracted from cell-free supernatant (50 mL) using ethyl acetate. The solvent was removed by rotary evaporation and the residue was re-dissolved in methanol (1 mL) and analyzed by HPLC and LC-HRMS (20 μL injection) with an Agilent Eclipse Plus C18 column (4.6 × 100 mm). A linear gradient of 2-95% CH_3CN (v/v) over 60 min in H_2O supplemented with 0.1% (v/v) TFA or formic acid at a flow rate of 0.5 mL/min was used for HPLC analysis or LC-HRMS analysis. LC-HRMS analysis was performed on an Agilent Technologies 6520 Accurate Mass QTOF LC-MS. HPLC analysis was performed on an Agilent 1260 HPLC with DAD. At least three independent replicates were performed, and representative results are shown.

Enzymatic synthesis of polyketides. Malonyl-CoA was made *in situ* with MatB using either sodium malonate or ^{13}C-1,3-labeled malonic acid. A typical reaction contained 100 mM HEPES (pH 8.0), 2 mM $MgCl_2$, 1 mM TCEP, 20 mM ATP, 100 mM fatty acids, 5 mM CoA, 20 mM sodium malonate, 20 μM Orf35, 10 μM HsPKS1, and 10 μM MatB. After overnight incubation, the proteins were precipitated using a final concentration of 5% (v/v) of TCA. **3** was purified using HPLC through an Intertsil ODS-4 column (4.6 mm i.d., 250 mm L, GL Sciences Inc.) with an isocratic program of 20% CH_3CN (v/v) over 30 min followed by 5 min in 95% CH_3CN with 0.1% (v/v) TFA at a flow rate of 1 mL/min. Fractions containing **3** were collected manually, concentrated under vacuum, and dried to white solid using a lyophilizer. NMR spectra of **3** were recorded on a Bruker Biospin 900 MHz spectrometer with a cryoprobe in *d6*-dimethyl sulfoxide (*d6*-DMSO; Cambridge Isotope Laboratories). **4** was purified and characterized in a similar way.

Biosynthesis of 5 in *E. coli*. BAP1/pACYC_antE-antM + pCDF_antD-antGF + pXZ53 + pXZ51, BAP1/pACYC_antE-antM + pCDF_antD-antGF + pXZ53 + pXZ52, BAP1/pACYC_antE-antM + pCDF_antD-antGF + pCOLADuet-1 empty vector + pXZ52 cells were grown in 500 mL of LB medium with 100 μg/mL carbenicillin, 100 μg/mL spectinomycin, 60 μg/mL kanamycin and 25 μg/mL chloramphenicol at 37 °C to an OD_{600} of 0.4-0.6. Subsequently, the cultures were supplemented with 0.5 mM IPTG, 1 mM anthranilic acid, and 1 mM 5-hexenoic acid. After 48 h of growth at 20 °C, the culture broth and the cell pellets were separated by centrifugation. Antimycins were extracted from cell-free supernatant (500 mL) using ethyl acetate. The solvent was removed by rotary evaporation and the residue was re-dissolved in methanol (0.5 mL) and analyzed by LC-HRMS (20 μL injection). LC-HRMS analysis was performed on an Agilent Technologies 6520 Accurate Mass QTOF LC-MS with an Agilent Eclipse Plus C18 column (4.6 × 100 mm). A linear gradient of 25-95% CH_3CN (v/v) over 20 min in H_2O with 0.1% (v/v) formic acid at a flow rate of 0.5 mL/min was used. At least three independent replicates were performed, and representative results are shown.

Large-scale production, purification and characterization of standard 5. The standard was synthesized through PDB by feeding 1 mM anthranilic acid and 1 mM 7-octynoic acid into JL1 strain that contained *antCDEFGM*[42]. The culture condition was same as described above. **5** was extracted from cell-free supernatant using ethyl acetate. The solvent was removed by rotary evaporation and the residue was re-dissolved in methanol. **5** was purified using HPLC through an Agilent Eclipse Plus C18 column (4.6 × 100 mm) with a linear gradient of 25-95% CH_3CN (v/v) over 20 min and 95% CH_3CN (v/v) for a further 5 min in H_2O with 0.025 % (v/v) TFA at a flow rate of 0.5 mL/min. Fractions containing **5** were collected manually, concentrated under vacuum, and dried to solid using a lyophilizer. LC-HRMS analysis was performed on an Agilent

Technologies 6520 Accurate Mass QTOF LC-MS with an Agilent Eclipse Plus C18 column (4.6 × 100 mm). A linear gradient of 25-95% CH_3CN (v/v) over 20 min in H_2O with 0.1 % (v/v) formic acid at a flow rate of 0.5 mL/min was used. LC-HRMS/MS analysis was performed using the same program described above with the target mass (m/z 417.2020 $[M+H]^+$) and a collision energy of 20 V around the retention time (15.6 min ± 1 min). NMR spectra of **5** were recorded on a Bruker Biospin 900 MHz spectrometer with a cryoprobe in *d4*-methanol (CD_3OD; Cambridge Isotope Laboratories).

Accession Codes

GenBank

scFadD and *scACP* (Accession number: KJ950369)

References

1 Bindman, N. A. & van der Donk, W. A. A general method for fluorescent labeling of the N-termini of lanthipeptides and its application to visualize their cellular localization. *J. Am. Chem. Soc.* **135**, 10362-10371 (2013).

2 Sin, N., Meng, L., Auth, H. & Crews, C. M. Eponemycin analogues: syntheses and use as probes of angiogenesis. *Bioorg. Med. Chem.* **6**, 1209-1217 (1998).

3 Harvey, C. J., Puglisi, J. D., Pande, V. S., Cane, D. E. & Khosla, C. Precursor directed biosynthesis of an orthogonally functional erythromycin analogue: selectivity in the ribosome macrolide binding pocket. *J. Am. Chem. Soc.* **134**, 12259-12265 (2012).

4 Ross, C., Scherlach, K., Kloss, F. & Hertweck, C. The Molecular Basis of Conjugated Polyyne Biosynthesis in Phytopathogenic Bacteria. *Angew. Chem. Int. Ed. Engl.* **53**, 7794-7798 (2014).

5 Thirumurugan, P., Matosiuk, D. & Jozwiak, K. Click chemistry for drug development and diverse chemical-biology applications. *Chem. Rev.* **113**, 4905-4979 (2013).

6 Sandy, M., Zhu, X., Rui, Z. & Zhang, W. Characterization of AntB, a promiscuous acyltransferase involved in antimycin biosynthesis. *Org. Lett.* **15**, 3396-3399 (2013).

7 Dupuis, S. N. *et al.* Synthetic diversification of natural products: semi-synthesis and evaluation of triazole jadomycins. *Chem. Sci.* **3**, 1640-1644 (2012).

8 Yan, Y. *et al.* Multiplexing of combinatorial chemistry in antimycin biosynthesis: expansion of molecular diversity and utility. *Angew. Chem. Int. Ed. Engl.* **52**, 12308-12312 (2013).

9 Martin, J. F., Casqueiro, J. & Liras, P. Secretion systems for secondary metabolites: how producer cells send out messages of intercellular communication. *Curr. Opin. Microbiol.* **8**, 282-293 (2005).

10 Minto, R. E. & Blacklock, B. J. Biosynthesis and function of polyacetylenes and allied natural products. *Prog. Lipid Res.* **47**, 233-306 (2008).

11 Yamaguchi, M., Park, H. J., Ishizuka, S., Omata, K. & Hirama, M. Chemistry and antimicrobial activity of caryoynencins analogs. *J. Med. Chem.* **38**, 5015-5022 (1995).

12 Shanklin, J., Guy, J. E., Mishra, G. & Lindqvist, Y. Desaturases: emerging models for understanding functional diversification of diiron-containing enzymes. *J. Biol. Chem.* **284**, 18559-18563 (2009).

13 Gagne, S. J., Reed, D. W., Gray, G. R. & Covello, P. S. Structural control of chemoselectivity, stereoselectivity, and substrate specificity in membrane-bound fatty acid acetylenases and desaturases. *Biochemistry* **48**, 12298-12304 (2009).

14 Haritos, V. S. *et al.* The convergent evolution of defensive polyacetylenic fatty acid biosynthesis genes in soldier beetles. *Nat. Commun.* **3**, 1150 (2012).

15 Blacklock, B. J., Scheffler, B. E., Shepard, M. R., Jayasuriya, N. & Minto, R. E. Functional diversity in fungal fatty acid synthesis: the first acetylenase from the Pacific golden chanterelle, Cantharellus formosus. *J. Biol. Chem.* **285**, 28442-28449 (2010).

16 Fritsche, K. *et al.* Biosynthetic genes and activity spectrum of antifungal polyynes from Collimonas fungivorans Ter331. *Environ. Microbiol.* **16**, 1334-1345 (2014).

17 Lee, M. *et al.* Identification of Non-Heme Diiron Proteins That Catalyze Triple Bond and Epoxy Group Formation. *Science* **280**, 915-918 (1998).

18 Edwards, D. J. *et al.* Structure and biosynthesis of the jamaicamides, new mixed polyketide-peptide neurotoxins from the marine cyanobacterium Lyngbya majuscula. *Chem. Biol.* **11**, 817-833 (2004).

19 Jones, A. C. *et al.* Genomic insights into the physiology and ecology of the marine filamentous cyanobacterium Lyngbya majuscula. *Proc. Natl. Acad. Sci. USA* **108**, 8815-8820 (2011).

20 Dorrestein, P. C. *et al*. Activity screening of carrier domains within nonribosomal peptide synthetases using complex substrate mixtures and large molecule mass spectrometry. *Biochemistry* **45**, 1537-1546 (2006).
21 Shanklin, J. & Cahoon, E. B. Desaturation and related modifications of fatty acids. *Annu. Rev. Plant Phys.* **49**, 611-641 (1998).
22 Zhang, W., Bolla, M. L., Kahne, D. & Walsh, C. T. A three enzyme pathway for 2-amino-3-hydroxycyclopent-2-enone formation and incorporation in natural product biosynthesis. *J. Am. Chem. Soc.* **132**, 6402-6411 (2010).
23 Wada, H., Avelange-Macherel, M. H. & Murata, N. The desA gene of the cyanobacterium Synechocystis sp. strain PCC6803 is the structural gene for delta 12 desaturase. *J. Bacteriol.* **175**, 6056-6058 (1993).
24 Nakamura, M. T. & Nara, T. Y. Structure, function, and dietary regulation of delta6, delta5, and delta9 desaturases. *Annu. Rev. Nutr.* **24**, 345-376 (2004).
25 Wada, H., Schmidt, H., Heinz, E. & Murata, N. In vitro ferredoxin-dependent desaturation of fatty acids in cyanobacterial thylakoid membranes. *J. Bacteriol.* **175**, 544-547 (1993).
26 Thompson, G. A. *et al*. Primary structures of the precursor and mature forms of stearoyl-acyl carrier protein desaturase from safflower embryos and requirement of ferredoxin for enzyme activity. *Proc. Natl. Acad. Sci. USA* **88**, 2578-2582 (1991).
27 Shanklin, J. & Somerville, C. Stearoyl-acyl-carrier-protein desaturase from higher plants is structurally unrelated to the animal and fungal homologs. *Proc. Natl. Acad. Sci. USA* **88**, 2510-2514 (1991).
28 Yin, J., Lin, A. J., Golan, D. E. & Walsh, C. T. Site-specific protein labeling by Sfp phosphopantetheinyl transferase. *Nat. Protoc.* **1**, 280-285 (2006).
29 Morita, H. *et al*. Synthesis of unnatural alkaloid scaffolds by exploiting plant polyketide synthase. *Proc. Natl. Acad. Sci. USA* **108**, 13504-13509 (2011).
30 Pfeifer, B. A., Admiraal, S. J., Gramajo, H., Cane, D. E. & Khosla, C. Biosynthesis of complex polyketides in a metabolically engineered strain of E. coli. *Science* **291**, 1790-1792 (2001).
31 Zhang, W., Li, Y. & Tang, Y. Engineered biosynthesis of bacterial aromatic polyketides in Escherichia coli. *Proc. Natl. Acad. Sci. USA* **105**, 20683-20688 (2008).
32 Shimo, T., Matsuzaki, S. & Somekawa, K. Intramolecular photoreactions of 6-(ω-alkenyl)-4-methoxy-2-pyrones. *J. Heterocycl. Chem.* **31**, 387-390 (1994).
33 Wilson, M. C. & Moore, B. S. Beyond ethylmalonyl-CoA: the functional role of crotonyl-CoA carboxylase/reductase homologs in expanding polyketide diversity. *Nat. Prod. Rep.* **29**, 72-86 (2012).
34 Sandy, M., Rui, Z., Gallagher, J. & Zhang, W. Enzymatic synthesis of dilactone scaffold of antimycins. *ACS Chem. Biol.* **7**, 1956-1961 (2012).
35 Pyke, K. A. Plastid division and development. *Plant Cell* **11**, 549-556 (1999).
36 Shanklin, J., Whittle, E. & Fox, B. G. Eight histidine residues are catalytically essential in a membrane-associated iron enzyme, stearoyl-CoA desaturase, and are conserved in alkane hydroxylase and xylene monooxygenase. *Biochemistry* **33**, 12787-12794 (1994).
37 Shieh, P., Hangauer, M. J. & Bertozzi, C. R. Fluorogenic azidofluoresceins for biological imaging. *J. Am. Chem. Soc.* **134**, 17428-17431 (2012).
38 Shieh, P., Siegrist, M. S., Cullen, A. J. & Bertozzi, C. R. Imaging bacterial peptidoglycan with near-infrared fluorogenic azide probes. *Proc. Natl. Acad. Sci. USA* **111**, 5456-5461 (2014).
39 Grammel, M. & Hang, H. C. Chemical reporters for biological discovery. *Nat. Chem. Biol.* **9**, 475-484 (2013).
40 Neef, A. B. & Luedtke, N. W. Dynamic metabolic labeling of DNA in vivo with arabinosyl nucleosides. *Proc. Natl. Acad. Sci. USA* **108**, 20404-20409 (2011).

41 Torella, J. P. *et al*. Tailored fatty acid synthesis via dynamic control of fatty acid elongation. *Proc. Natl. Acad. Sci. USA.* **110**, 11290-11295 (2013).

42 Liu, J., Zhu, X., Seipke, R. F. & Zhang, W. Biosynthesis of Antimycins with a Reconstituted 3-Formamidosalicylate Pharmacophore in Escherichia coli. *ACS Synth. Biol.* doi:10.1021/sb5003136 (2014).

Figure 1

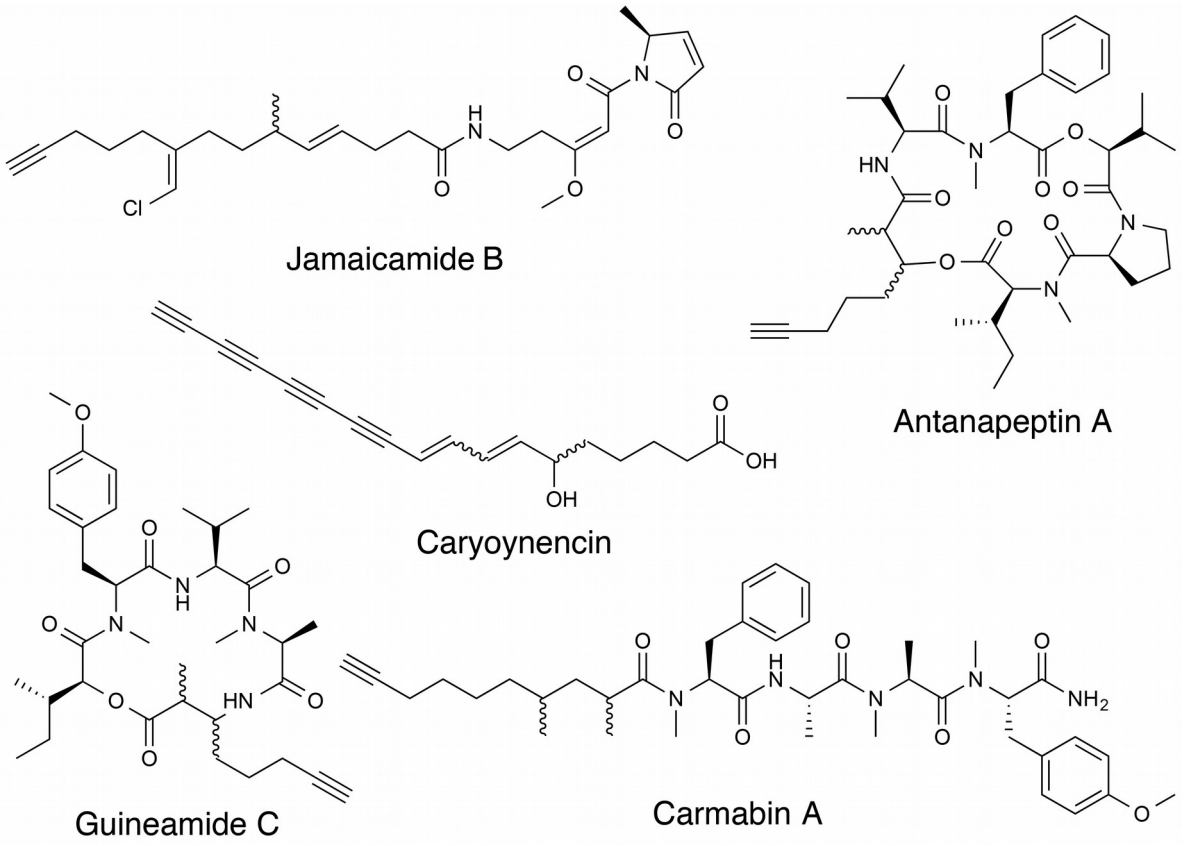
Jamaicamide B
Antanapeptin A
Caryoynencin
Guineamide C
Carmabin A

Figure 2

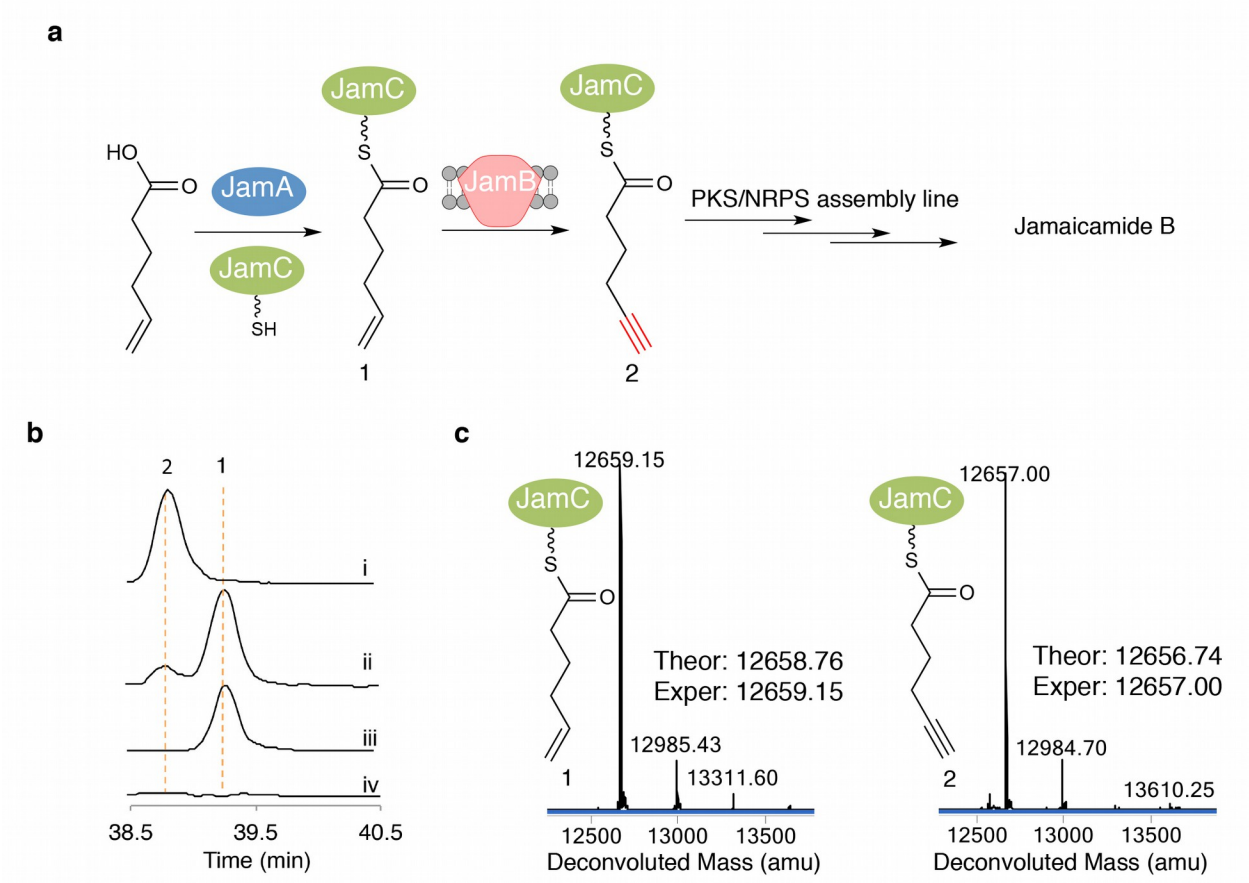
a
HO
O
JamA
JamC
SH
JamC
S
O
1
JamB
JamC
S
O
2
PKS/NRPS assembly line
Jamaicamide B
b
2
1
i
ii
iii
iv
38.5
39.5
40.5
Time (min)
c
12659.15
JamC
S
O
Theor: 12658.76
Exper: 12659.15
12985.43
1
13311.60
12500
13000
13500
Deconvoluted Mass (amu)
12657.00
JamC
S
O
Theor: 12656.74
Exper: 12657.00
12984.70
2
13610.25
12500
13000
13500
Deconvoluted Mass (amu)

Figure 3

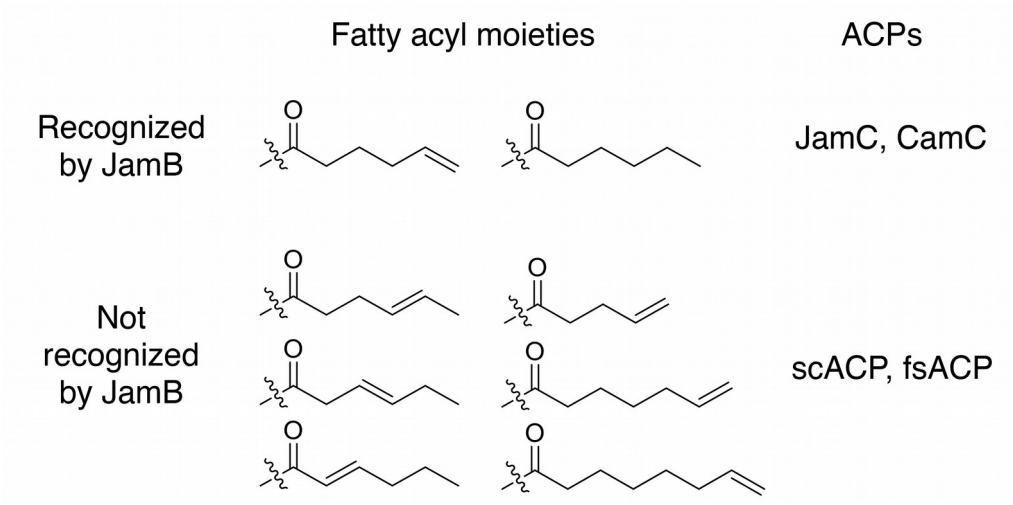
Fatty acyl moieties
ACPs
Recognized by JamB
JamC, CamC
Not recognized by JamB
scACP, fsACP

Figure 4

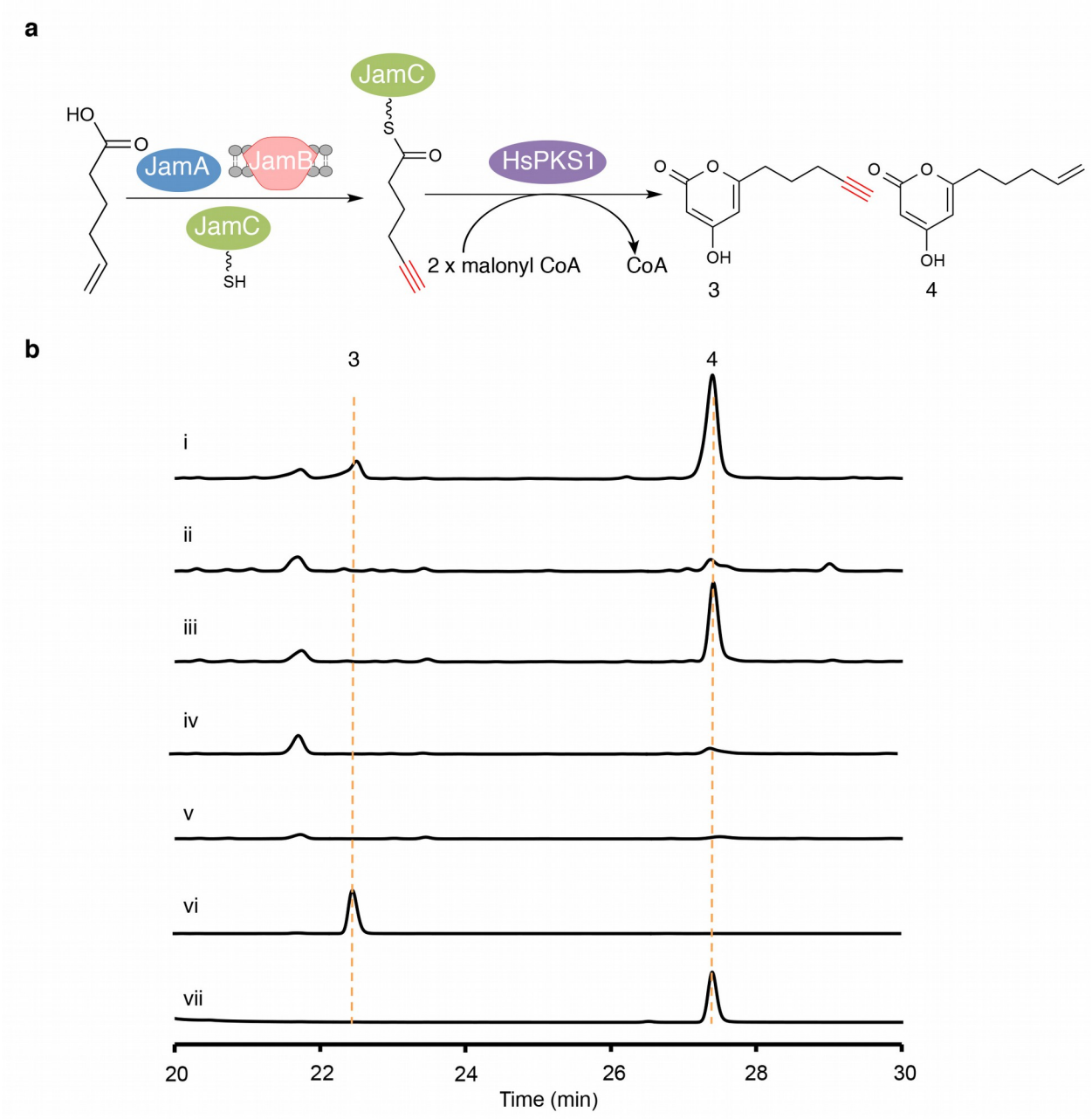
a
HO
O
JamA
JamB
JamC
SH
JamC
S
O
HsPKS1
2 x malonyl CoA
CoA
O
O
OH
3
O
O
OH
4
b
3
4
i
ii
iii
iv
v
vi
vii
20
22
24
26
28
30
Time (min)

Figure 5

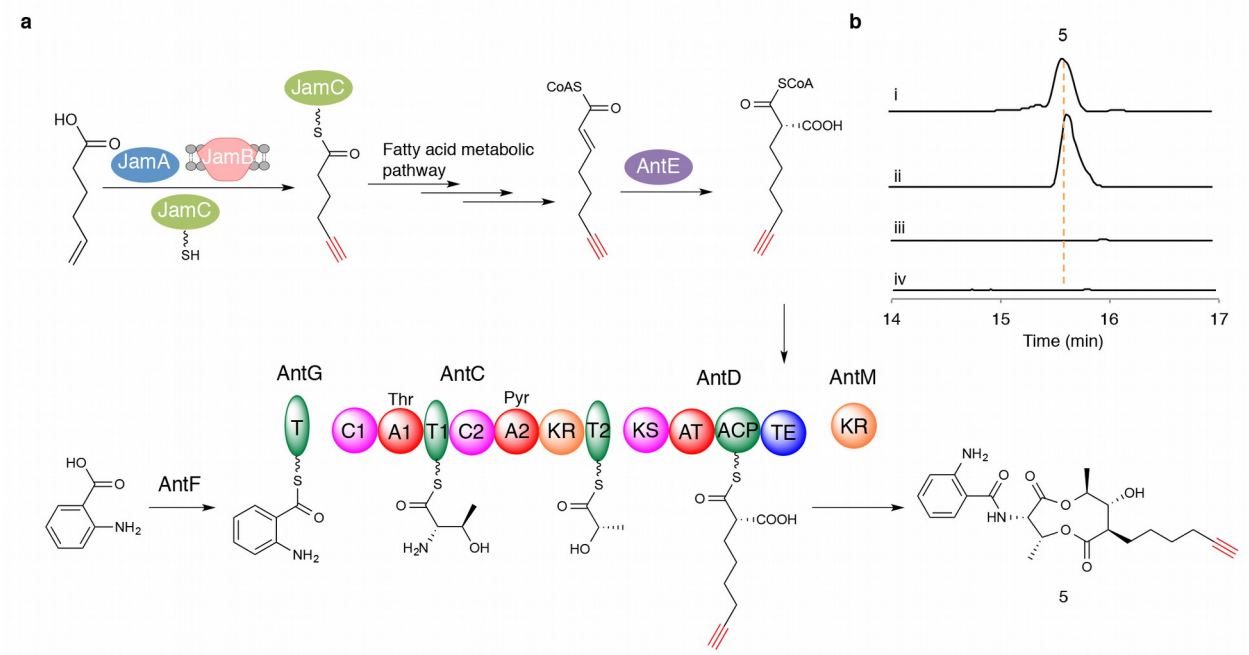
a
b
JamA
JamB
JamC
JamC
SH
Fatty acid metabolic pathway
CoAS
AntE
SCoA
COOH
5
i
ii
iii
iv
14
15
16
17
Time (min)
AntF
AntG
AntC
AntD
AntM
T
C1
A1
Thr
T1
C2
A2
Pyr
KR
T2
KS
AT
ACP
TE
KR
NH2
OH
COOH
HN
5